CEBAF Program Advisory Committee Ten Proposal Cover Sheet

This document must be received by close of business on Tuesday, December 19, 1995 at:

CEBAF

User Liaison Office, Mail Stop 12 B

12000 Jefferson Avenue

Newport News, VA 23606

(Choose one)

☑ **New Proposal Title:** Precision Measurement of the nucleon spin structure functions in the Region of the Nucleon Resonances

☐ **Update Experiment Number:**

☐ **Letter-of-Intent Title:**

Contact Person

Name: Steve A Rawson

Institution: University of Virginia Nuclear Physics Laboratory

Address: Physics Department

Address: McCormick Road

City, State ZIP/Country: Charlottesville, VA 22901

Phone: (804) 924-6757 **FAX:** (804) 924-4576

E-Mail → Internet: sar6v@virginia.edu

Experimental Hall: C **Days Requested for Approval:** 21

CEBAF Use Only

Receipt Date: 12/19/95 PR 95-005

By: gp

LAB RESOURCES REQUIREMENTS LIST

CEBAF Proposal No.: _____ Date: _____
(For CEBAF User Liaison Office use only.)

List below significant resources — both equipment and human — that you are requesting *from CEBAF* in support of mounting and executing the proposed experiment. Do not include items that will be routinely supplied to all running experiments, such as the base equipment for the hall and technical support for routine operation, installation, and maintenance.

Major Installations *(either your equip. or new equip. requested from CEBAF)*

_____

_____

_____

_____

_____

_____

_____

_____

_____

New Support Structures: _____

_____

_____

Data Acquisition/Reduction

Computing Resources: _____

_____

_____

New Software: _____

_____

_____

Major Equipment

Magnets _____

_____

Power Supplies _____

_____

Targets _____

_____

Detectors _____

_____

Electronics _____

_____

Computer Hardware _____

_____

Other _____

_____

Other

_____

_____

_____

_____

_____

HAZARD IDENTIFICATION CHECKLIST

CEBAF Experiment: _____ Date: _____

Check all items for which there is an anticipated need—do not check items that are par of the CEBAF standard experiment (HRSE, HRSH, CLAS, HMS, SOS in standar configurations).

Cryogenics
- _____ beamline magnets
- _____ analysis magnets
- ✓ target
- _____ drift chambers
- _____ other

Electrical Equipment
- _____ cryo/electrical devices
- _____ capacitor banks
- _____ high voltage
- _____ exposed equipment

Radioactive/Hazardous Materials
List any radioactive or hazadorous/ toxic materials planned for use:
NH3, ND3 ... T ...
...

Pressure Vessels
- _____ inside diameter
- _____ operating pressure
- _____ window material
- _____ window thickness

Flammable Gas or Liquids
(incl. target)
- type: _____
- flow rate: _____
- capacity: _____

Other Target Materials
- ___ Beryllium (Be)
- ___ Lithium (Li)
- ___ Mercury (Hg)
- ___ Lead (Pb)
- ___ Tungsten (W)
- ___ Uranium (U)
- ___ Other (list below)

_____
_____

Vacuum Vessels
- _____ inside diameter
- _____ operating pressure
- _____ window material
- _____ window thickness

Radioactive Sources
- _____ permanent installation
- _____ temporary use
- type: _____
- strength: _____

Large Mech. Structure/System
- _____ lifting devices
- _____ motion controllers
- _____ scaffolding or elevated platforms
- _____ other

Lasers
- type: _____
- wattage: _____
- class: _____

Installation
- _____ permanent
- _____ temporary

Use
- _____ calibration
- _____ alignment

Hazardous Materials
- ___ cyanide plating materials
- ___ scintillation oil (from)
- ___ PCBs
- ___ methane
- ___ TMAE
- ___ TEA
- ___ photographic developers
- ✓ other (list below)

...
(... target)
...

Notes:

BEAM REQUIREMENTS LIST

CEBAF Proposal No.: _____ Date: _____
(For CEBAF User Liaison Office use only.)

List all combinations of anticipated targets and beam conditions required to execute the experiment. (This list will form the primary basis for the Radiation Safety Assesment Document (RSAD) calculations that must be performed for each experiment.)

Condition #	Beam Energy (MeV)	Beam Current (μA)	Polarization and Other Special Requirements (e.g., time structure)	Target Material (use multiple rows for complex targets — e.g., w/windows)	Target Material Thickness (mg/cm²)
1	6 000	≥ 5.0 6	≥ 80 % long. Tarjet / Tolerant	NH_3	
				^4He	

The beam energies, E_{Beam}, available are: $E_{Beam} = N \times E_{Linac}$ where N = 1, 2, 3, 4, or 5. For 1995, E_{Linac} = 800 MeV, i.e., available E_{Beam} a 800, 1600, 2400, 3200, and 4000 MeV. Starting in 1996, in an evolutionary way (and not necessarily in the order given) the followi additional values of E_{Linac} will become available: E_{Linac} = 400, 500, 600, 700, 900, 1000, 1100, and 1200 MeV. The sequence a timing of the available resultant energies, E_{Beam}, will be determined by physics priorities and technical capabilities.

CEBAF PROPOSAL

Precision measurement of the nucleon spin structure functions in the region of the nucleon resonances

D.G. Crabb, C. Cothran, D. Day, E. Frlez, J. S. McCarthy,

P. McKee, D. Počanić, C. Smith,

O. Rondon-Aramayo (spokesman) and A. Tobias

Institute of Nuclear and Particle Physics

Department of Physics, University of Virginia

Charlottesville, VA 22901, USA

J. Jourdan and I. Sick,

two research associates and students

Institut für Physik, Universität Basel, CH-4056, Basel, Schweiz

R. Carlini, J-P. Chen, J. Gomez, D. Mack,

J. Mitchell, C. Sinclair

Continuous Electron Beam Accelerator Facility

Newport News, VA, 23606

Abstract

We propose to make high precision and high resolution measurements of the spin structure of the proton and deuteron in the region of the nucleon resonances, at two values of Q^2: ~ 1 GeV^2 and ~ 5.5 GeV^2. Fundamental properties of the nucleon and QCD will be explored with adequate precision to obtain conclusive information. We plan to use CEBAF's polarized electron beam at 6 GeV, the Virginia-Basel solid polarized target with NH_3 and ND_3 materials and the Hall C High Momentum Spectrometer.

1. Motivation

The availability of polarized electron beams of 6 GeV or higher energies at CEBAF, substantially broadens the opportunities of physics experiments with polarized beams and targets. In particular, it opens up the feasibility of extending the studies of the nucleon spin structure beyond the D.I.S. region that is under current scrutiny in experiments at SLAC [1,2], CERN [3] and HERA [4], into the little known nucleon resonances region, for which only one set of data is currently available [5]. The extensive past studies of the DIS nucleon spin structure functions at SLAC [6–12] and CERN [13,14], have firmly established that the fraction of the proton spin carried by the quarks is 30%±5%. Our understanding of the nucleon spin for final state invariant mass $W < 2$ GeV is far less certain. New results from the low energy (9.7 GeV) data of SLAC Experiment 143 are expected to make limited improvements on our existing knowledge, due to lack of spectrometer resolution.

The objective of the experiment described in this proposal is to measure in detail the spin asymmetries for both the proton and the deuteron in the region of the nucleon resonances at two values of Q^2, combining the proven solid polarized target technology used at SLAC in E143, with the advantages offered by CEBAF's Hall C High Momentum Spectrometer (HMS), and the beam's unity duty factor, using essentially the same setup as that of Hall C experiments 93-026 [21] and 93-028 [22]. These advantages are:

- A much greater solid angle than the dedicated SLAC End Station A (ESA) spectrometers used in E142/E143 [23]. The ratio is 15 to 1 for the ESA 7° spectrometer and 60 to 1 for the 4.5° one.

- A much improved momentum resolution for the HMS ($dp/p = 0.3\%$), compared to the $\sim\geq 2\%$ resolution in the high Bjorken x range at SLAC.

- No count rate limitations due to high instantaneous current. A 100 nA average current, which is the highest that the polarized target has been shown to tolerate and still operate reliably, corresponds to a 4200 times larger: 420 μA/(2μs pulse) instantaneous current at

FIGURES

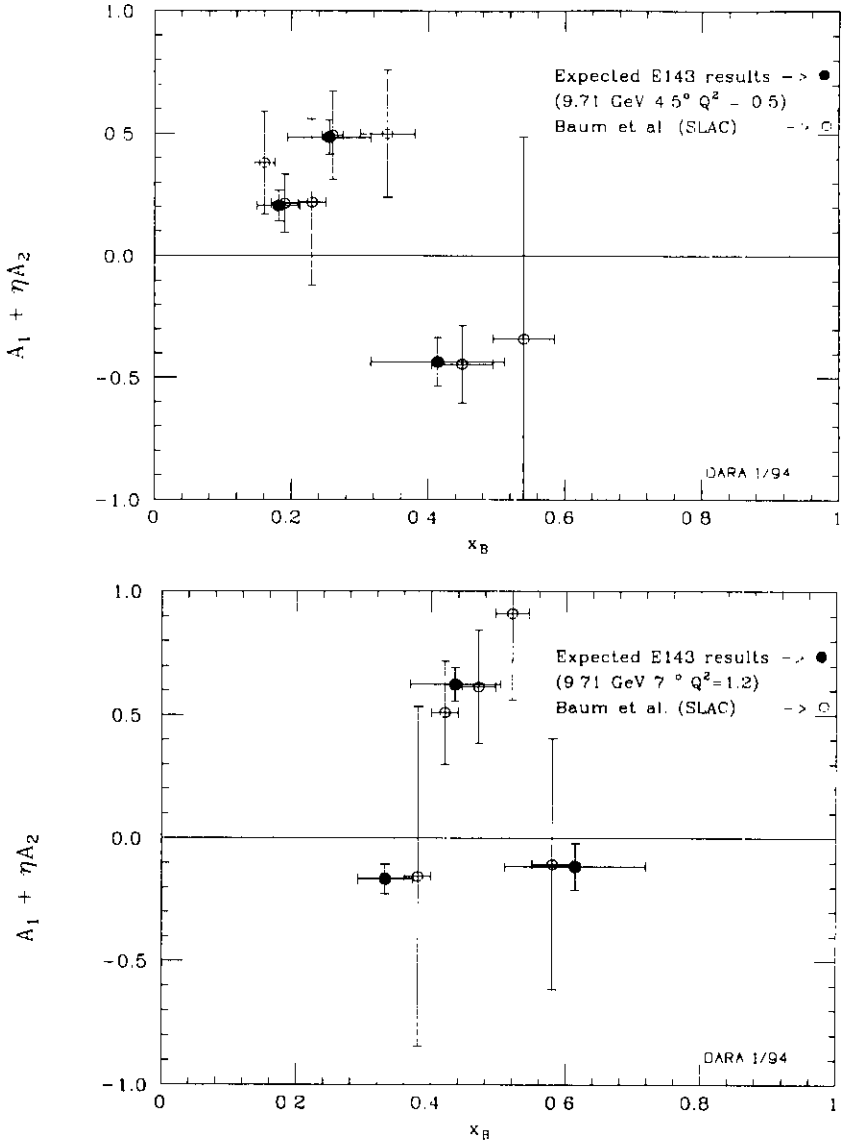

FIG. 1. The proton spin asymmetries $A_1 + \eta A_2$ in the nucleon resonances region, current data (open circles) and expected E143 results (black circles).

SLAC. This restriction limited E143 data taking at 9.7 GeV to equivalent average beam currents of only $\sim$ 25 nA.

The smaller momentum bite of the HMS ($\pm 10\%$) compared to that of the SLAC spectrometers ($\pm 100\%$), is not of major concern, since the region of interest can be covered with at most two settings, at any angle. Moreover, it could be compensated in part by choosing a tune that sacrifices some resolution for a broader bite, since a 0.3% dp/p resolution is quite

satisfactory.

The present spin asymmetry data on the resonances region are old [5] and have large uncertainties, while the expected results from E143 have marginal resolution. The situation is illustrated graphically in Fig.1. In spite of E143's good statistical uncertainties, in that experiment the W range from the pion production threshold to the upper end of the third resonance region cannot be resolved in better than three bins.

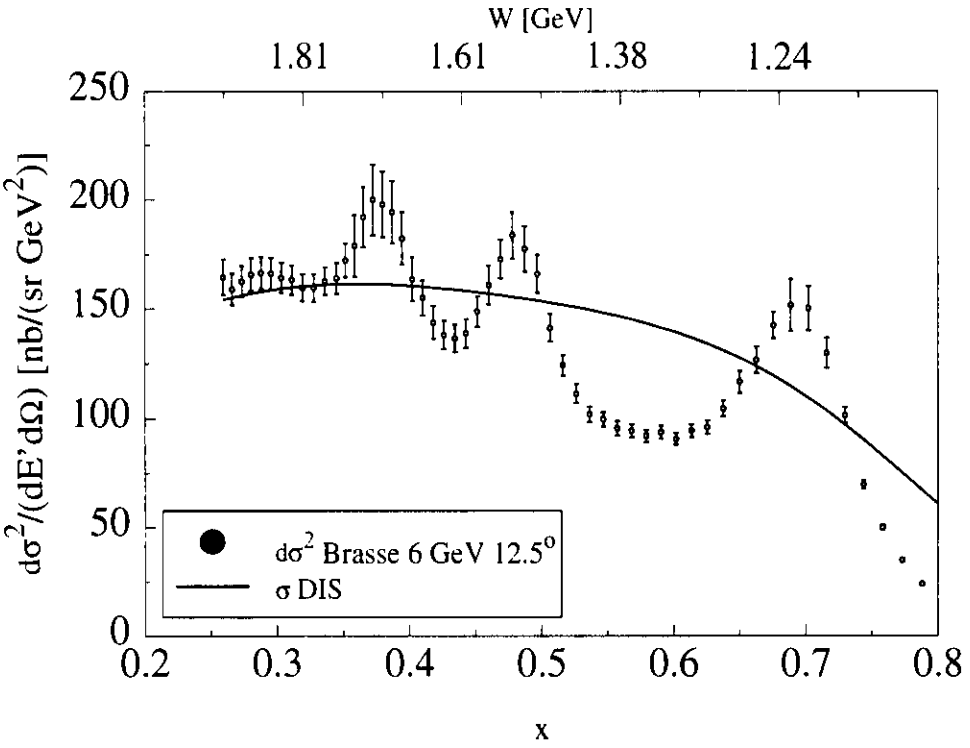

FIG. 2. The $e - p$ double differential cross section in the nucleon resonances region, at the resolution expected in CEBAF's Hall C. Also shown is the extrapolated DIS cross section.

On the other hand, a high resolution experiment using CEBAF's Hall C HMS could measure the spin asymmetries with equal or better uncertainties than those of E143 and with the resolution shown in Fig. 2, in about three weeks running time, for both protons and deuterons. The Virginia-Basel polarized target used in E143 is capable of polarizing both protons and deuterons, and its magnetic field can be oriented in a broad range of angles relative to the lepton helicity or to the the three-momentum transfer $\mathbf{q}$, for the study of both longitudinal and transverse asymmetries. This capability is fundamental for the

separation of the longitudinal (A_1) and transverse (A_2) components, which at low energy have comparable kinematic coefficients (see eq.(9)).

The knowledge that will be gained on A_1 and A_2 has, of course, fundamental bearing on our understanding of the properties of the nucleon and its excitations. A_1, like its DIS counterpart $g_1(x)$ is related to the spin composition of the nucleon. At high x, QCD predicts that A_1 approaches 1: the leading quark carries all the spin. This behavior has only been tested up to $x = 0.8$ at $Q^2 \simeq 10$ GeV^2 in E143, with substantial uncertainties due to low counting rates. The computation of the moments of the spin structure functions to test sum rules such as the Bjorken sum rule [15] relies on extrapolations from $x = 0.8$ to $x = 1$ based on quark counting rules [16]. Measuring the asymmetries in the resonances region would also test if such extrapolations for the asymmetries agree with the local (Bloom-Gilman [17]) duality observed for the unpolarized cross sections. Since the range $0.8 < x < 1$ corresponds to the resonances region for $Q^2 < 12$ GeV^2, the counting rate conditions favor CEBAF experiments at this kinematics.

A_2 is related to $g_2(x)$, which has a significant contribution from twist-3 matrix elements that describe quark-gluon interactions [18,19]. CEBAF is a unique facility to study the low Q^2 properties of this fundamental asymmetry, which has been measured at SLAC [12] and CERN [20] at much higher Q^2, with poor precision and only in the low and intermediate x region. The current HERMES experiment has similar kinematics as E143 and is not expected to contribute A_2 data at low Q^2.

The improvements in our understanding of the spin structure of the nucleon resonances that would result from this experiment, will have a positive impact in a wide range of areas of fundamental nuclear physics. They would range from additional confirmation of the M_1 magnetic dipole nature of the transition in the region of the $\Delta(1232)$ resonance, that in polarized inclusive scattering is based on the lone point at $x = 0.45$ in the $Q^2 = 0.5$ GeV^2 part of fig.1, to valuable complementary data on the asymmetries in a region of Q^2 where the extended Gerasimov-Drell-Hearn [24] sum rule

$$I(Q^2) = \int_{Q^2/2m\nu}^{\infty} g_1^p(\nu, Q^2)\frac{d\nu}{\nu} = \frac{2m^2}{Q^2}\int_0^1 g_1^p(x, Q^2)dx = \Gamma(Q^2) \qquad (1)$$

that will be measured at CEBAF [25–27] is expected to have a change of sign. The data at high Q^2 would provide unambiguous information on the validity of the pQCD prediction [28] that the electric quadrupole transition E_2 becomes comparable to M_1 in that kinematic regime. These results also would find application in more technical but still very important areas like the radiative corrections for polarized electrons scattering on polarized targets, for which the main source of error comes from the lack of data in the resonance region. In summary, this experiment would yield major physics results for a minimal investment in beam time.

2. Polarized lepton scattering formalism

When longitudinally polarized leptons are incident on polarized nuclei one can compute the sum and the difference of the cross sections for two opposing orientations θ_N and $\theta_N + \pi$ of the nucleon spin. The sum is just twice the unpolarized cross section, while the difference [29], [30] is sensitive to the nucleon polarization. For $\theta_N = 0$ (i.e. longitudinally polarized leptons and nucleons) we get

$$\frac{d^2\sigma(0)}{d\Omega dE'} - \frac{d^2\sigma(\pi)}{d\Omega dE'} = \sigma^{\uparrow\uparrow} - \sigma^{\uparrow\downarrow} = \frac{4\alpha^2 E'}{Q^4 E}((E + E'\cos\theta)MG_1(\nu, Q^2) - Q^2 G_2(\nu, Q^2)) \qquad (2)$$

and for $\theta_N = \pi/2$ (longitudinal leptons and transverse nucleons) the result is

$$\frac{d^2\sigma(\pi/2)}{d\Omega dE'} - \frac{d^2\sigma(3\pi/2)}{d\Omega dE'} = \sigma^{\uparrow\rightarrow} - \sigma^{\uparrow\leftarrow} = \frac{4\alpha^2 E'}{Q^4 E}E'\sin\theta(MG_1(\nu, Q^2) + 2EG_2(\nu, Q^2)) \qquad (3)$$

where θ is the lepton scattering angle, Ω is the lepton detector solid angle, M is the nucleon mass, and $\nu = E - E'$ is the energy transfer; E and E' are the beam and final electron energies.

$G_1(\nu, Q^2)$ and $G_2(\nu, Q^2)$ are the spin structure functions. They can be related in the asymptotic limit to helicity distributions of the partons in the nucleon:

$$\lim_{Q^2,\nu\to\infty}(M\nu)MG_1(\nu, Q^2) = g_1(x), \qquad \lim_{Q^2,\nu\to\infty}(M\nu)\nu G_2(\nu, Q^2) = g_2(x). \qquad (4)$$

that are functions of the Bjorken scaling variable $x = Q^2/(2M\nu)$.

An equivalent approach can be followed starting from the virtual photon absorption cross sections for photon helicities +1, -1, 0: $\sigma^T_{1/2}, \sigma^T_{3/2}, \sigma^{TL}_{1/2}$, from which the spin asymmetries A_1, A_2 are constructed:

$$A_1 = \frac{\sigma^T_{1/2} - \sigma^T_{3/2}}{\sigma^T_{1/2} + \sigma^T_{3/2}} = \frac{M\nu G_1(\nu, Q^2) - Q^2 G_2(\nu, Q^2)}{W_1(\nu, Q^2)} \tag{5}$$

$$A_2 = \frac{\sigma^{TL}}{\sigma^T} = \frac{\sqrt{Q}(MG_1(\nu, Q^2) + \nu G_2(\nu, Q^2))}{W_1(\nu, Q^2)} \tag{6}$$

where $\sigma^T = \sigma^T_{3/2} + \sigma^T_{1/2}$. This approach involves the unpolarized structure function $W_1(\nu, Q^2) = (W^2 - M^2)\sigma^T/(8M\pi\alpha^2)$, which must be obtained from the more accessible ones $\nu W_2(\nu, Q^2) = F_2(\nu, Q^2)$ and $R(x, Q^2) = \sigma_L/\sigma_T$ using $W_1/W_2 = (1 + \nu^2 Q^2)/(1 + R)$.

The spin asymmetries are related to the measured asymmetries for the longitudinal and transversal configurations of the beam and target spins (known as $A_{||}$ and $A_\perp$, $A = (\sigma^{\uparrow\uparrow} - \sigma^{\uparrow\downarrow})/(\sigma^{\uparrow\uparrow} + \sigma^{\uparrow\downarrow})$) by expressions that involve kinematical factors, as well as the unpolarized structure function $R(x, Q^2)$.

$$A_1 = \frac{C}{D}\left(A_{||} - dA_\perp\right) \tag{7}$$

$$A_2 = \frac{C}{D}\left(c'A_{||} + d'A_\perp\right) \tag{8}$$

where $C = 1/(1 + \eta c')$, $\eta = \epsilon\sqrt{Q^2}/(E - \epsilon E')$, $c' = \eta(1 + \epsilon)/(2\epsilon)$, $\epsilon^{-1} = 1 + 2[1 + (\nu^2/Q^2)]\tan^2(\theta/2)$ is the usual longitudinal polarization of the virtual photon, $D = (1 - \epsilon E'/E/)/(1 + \epsilon R)$ is the virtual photon depolarization factor which is a function of R, $d' = 1/\sqrt{2\epsilon/(1 + \epsilon)}$ and $d = \eta d'$.

Experiments that measure only $A_{||}$ cannot separate A_1 and A_2, unless additional measurements with different beam energies at the same scattering angle are made, since both spin asymmetries are related to $A_{||}$ by

$$A_{||} = D(A_1 + \eta A_2). \tag{9}$$

The coefficient η ranges from $\sim$ 1 at W = 1.17 GeV to $\sim$ 0.35 at W = 2 GeV, so the contribution of A_2 cannot be neglected. The recent results from E143 [12] indicate that A_2 is $\sim 0.12 A_1$ for Q^2 = 3 GeV^2, $0.53 < x < 0.75$ and shows no Q^2 dependence, within uncertainties. Although the E143 results apply to the deep inelastic region, we can use the average ratio A_2/A_1 at these high x values to estimate that the total A_2 contribution to $A_{||}$ may be $\geq$ 12%.

3. Test of perturbative QCD

A very interesting application of the asymmetries data to be measured at high Q^2 in this experiment is the testing of the pQCD prediction concerning helicity conservation in the N-Δ (1232) transition [28]. Past studies of the Q^2 dependence of the transition form factors for this and other resonances [31,32] are not conclusive, although there are indications that the form factors for the second and third resonance regions approach the pQCD behavior at $Q^2 >$ 3 GeV^2, while the Δ shows a faster decrease than the Q^{-4} expected dependence.

Large statistical uncertainties due to low count rates at high Q^2 and contributions from non-resonant processes complicate the extraction of the form factors in inclusive experiments. An exclusive experiment to measure the form factors up to Q^2= 6 GeV^2 has been approved to run in Hall B [33]. A similar experiment restricted to the Δ and Q^2= 4 GeV^2 has also been approved for Hall C [34]. In both cases, unpolarized beam and targets are contemplated. In the present case, the use of polarization degrees of freedom provides a powerful handle to explore the properties of the relevant amplitudes (helicity or multipole).

As illustrated in more detail in the Appendix, the asymmetry for photo- or electroproduction of the Δ is expected to approach -1 in the perturbative regime. This is due to the electric quadrupole form factor E_2 (or E_{1+}) becoming dominant: $E_2 = \sqrt{3}M_1$, because a double spin flip is involved in the process $N_{1/2} + \gamma_{-1} \rightarrow \Delta_{-3/2}$, where the subscripts refer to the helicities of the particles. This process is described by the helicity amplitude $G_- = \sqrt{4\pi}(-\sqrt{3}M_1 + E_2)/2$, which is strongly suppressed by helicity conservation. (The asymptotic relation between the multipoles is obtained by setting $G_- = 0$). A measurement of the related asymmetry A_{TT} (displayed in detail in the Appendix) to a precision of $\sim$0.1

(absolute) would be a conclusive test ($\simeq$10% relative) if the asymmetry is of order unity, and would establish a reasonable upper bound for the E_2/M_1 ratio at the proposed Q^2= 5.7 GeV^2, if the perturbative regime turns out to set in only at higher momentum transfers.

The example in the Appendix is limited to the the case of the Δ resonance, but it can readily be extended to the other resonances for which the asymmetry at high Q^2 can be measured at the same momentum setting of the spectrometer. These high Q^2 studies would yield high physics benefits for a minimal cost of additional beam time.

4. Kinematic coverage

As we can see from Fig. 3, the nucleon resonances region covers a very large fraction of the x range for low beam energies, such as the 9.7 GeV case of E143. For the ESA 7° spectrometer, the kinematic region $0.2 \leq x \leq 1$ at $Q^2 \sim 1$ GeV^2 is accessible. This same region would be accessible at CEBAF's lower beam energies ($\leq$ 6 GeV) at a 12.5° angle. At greater scattering angles, higher Q^2 values are reachable, and the resonances move closer to $x = 1$, but the final energy interval

$$\frac{\Delta E'}{E'} = \frac{2(\ W_h{}^2 - \ W_l{}^2)}{2\,M^2 + 4\,EM - \ W_l{}^2 - \ W_h{}^2} \tag{10}$$

depends only on the invariant mass range $W_h - W_l$ and the beam energy E. For $E = 6$ GeV, $W_l = 0.938$ GeV ($= M$) and $W_h = 2$ GeV ($<Q^2>$ 1.3 Gev^2), $\Delta E'/E' = 0.32$, so two spectrometer settings are needed. For $E = 4$ GeV three settings are needed, making low Q^2 measurements less attractive, at any angle.

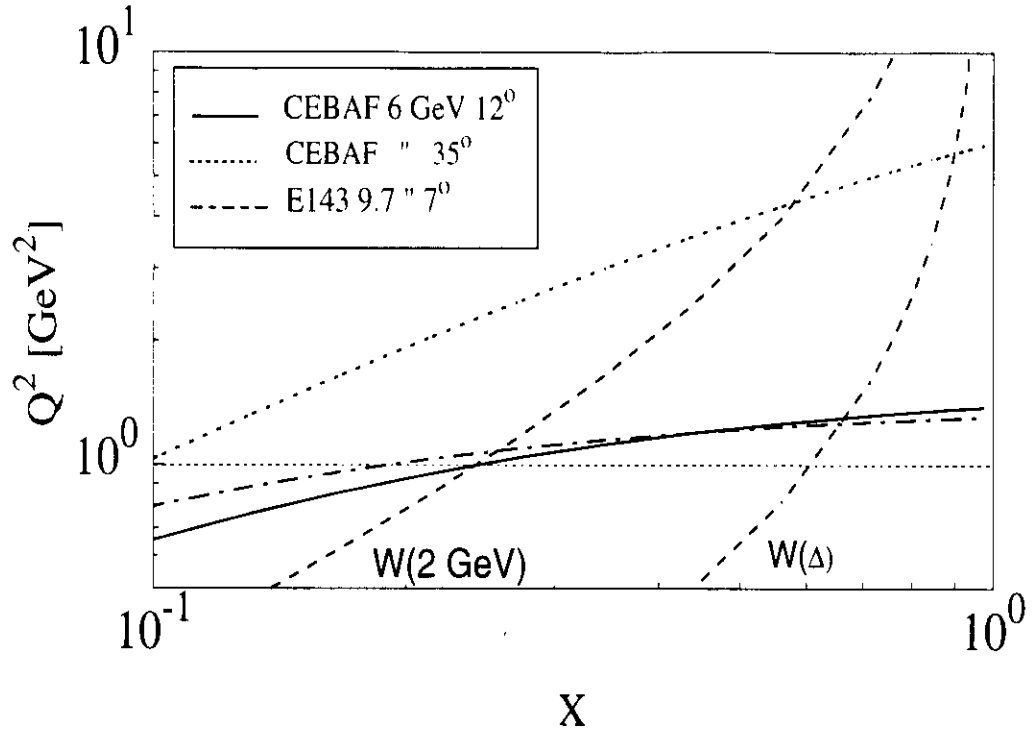

FIG. 3. The kinematic range accessible at 6 and 9.711 GeV beam energies and three angles. The long dashed curves are lines of constant W.

At 35° the average Q^2 is 5.22 GeV^2, but it is 5.7 GeV^2 at the top of the $\Delta(1232)$. This is a sufficiently high value of Q^2 to test the pQCD prediction. The momentum bite and the upper and lower limits of the final electron energy are related by

$$E'_l = E'_h \frac{1 - \frac{\Delta p}{p}}{1 + \frac{\Delta p}{p}}. \tag{11}$$

For $E'_h = 4.984$ GeV, (corresponding to the π production threshold, W_l =1.17 GeV) a value $E'_l = 4.130$ GeV, corresponding to W_h =1.83 GeV, is attainable at one momentum setting, so most of the three resonances region can be covered in a single run at 35°.

5. Experimental equipment.

The equipment needed to carry out the proposed experiment is summarized below:

- Polarized 6 GeV electron beam, $\geq$ 80% longitudinal polarization, 60 to 100 nA beam current.
- CEBAF's Hall C HMS spectrometer in a tune that combines a 10 msr solid angle, $\simeq$

0.3% momentum resolution and ± 10% momentum bite.

- The normal HMS detector package to identify electrons and reject pions.
- The Hall C Møller polarimeter.
- The Virginia-Basel polarized target, with ≥ 85 % NH_3 polarization and ≥ 30% ND_3 polarization.
- Data acquisition system (electronics, hardware and software) capable of ∼ 1 kHz event rate.

6. Count Rates and running times

The count rate of scattered electrons from the polarized target is given by

$$R = \frac{\mathcal{L}\mathcal{A}}{f}\frac{d\sigma^2}{d\Omega dE'} \tag{12}$$

where the luminosity $\mathcal{L} = 1 \times 10^{35}$ cm^{-2}Hz combines a 60 nA beam current with $\simeq 3 \times 10^{23}$ cm^{-2} thickness for the 3 cm long ^{15} NH_3 and ^{15} ND_3 solid polarized targets. The acceptance $\mathcal{A} = \Delta E'\Delta\Omega \simeq 0.2$ GeV msr corresponds to 15 MeV ΔW increments (which translate into $\Delta E' = 15$ MeV near the π threshold and $\Delta E' = 27$ MeV at $W = 1.95$ GeV) combined with the HMS solid angle $d\Omega = 10$ msr. The $e-p$ resonance scattering cross section $d\sigma^2/(d\Omega dE')$ is based on Brasse's [35] parameterization, and its corrected by the dilution factor f, which takes into account the fact that both polarized nucleons (3 H) and unpolarized nucleons (^{15}N, ^{4}He and other materials) are present in the target:

$$f = \frac{N_p\sigma_p}{N_p\sigma_p + N_{15N}\sigma_{15N} + N_{other}\sigma_{other}} \tag{13}$$

where $N_i = \rho_i m_i p_f$ is the number of nuclei of type i present in the target, ρ is the density of the material, m is the molecular weight, and p_f is the fraction of the target volume occupied by the material (packing fraction). The cross sections are per-nucleon $d\sigma^2(E,\theta)/(d\Omega dE')$ appropriate to the kinematic regime (resonances region). This implies that the neutron and proton cross sections are approximately the same, and that the dilution factor is close to $3/(3+15+\varepsilon)\approx 0.13$ where $\varepsilon \leq 5$ is the contribution of He and other materials.

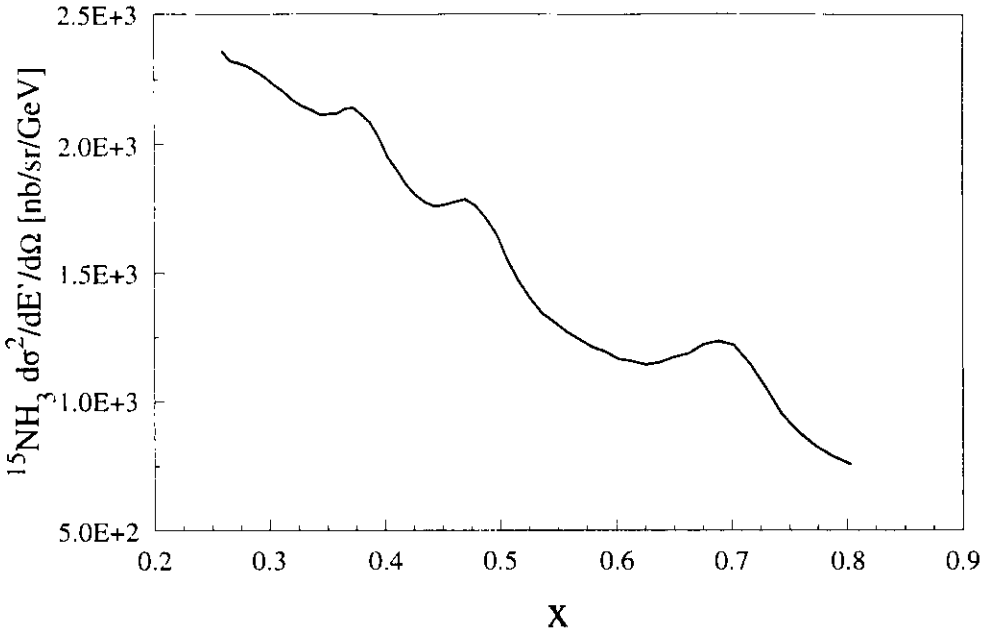

FIG. 4. Ammonia ($^{15}NH_3$) cross section from a combination of ^{15}N and 3 times the resonance $e-p$ cross section.

Of course, the presence of nitrogen and other materials in the target smears out the resonance shapes that stand out when the target is only hydrogen. Moreover, corrections must be applied to the measured asymmetries, to account for the small contribution of ^{15}N to the target polarization [9]. Fig. 4 shows a representative shape of the expected spectrum in the region of interest. The cross section for ammonia shown in this plot was constructed from a y-scaling model of ^{12}C [36] calculated for similar kinematic conditions ($E = 6$ GeV, $\theta = 13°$), and normalized to ^{15}N, plus three times the $e-p$ resonance cross section [35].

For deuterated ammonia $^{15}ND_3$ the definitions are similar, with the appropriate substitutions of D for p. The numerical value can be approximated by $6/(6+15+5)\approx 0.23$.

Table 1 presents representative values of the rates for the proton for different values of W. The cross section is from ref. [35], combined with a quasielastic tail contribution [36] that extends down to $x \sim 0.5$. Also shown is the extrapolated DIS cross section (displayed in fig.2) from SLAC's L.W. Whitlow [38,37] global fits to the unpolarized structure functions F_2 and R, which are appropriate for our chosen kinematics. The rates are for $\Delta W = 15$

MeV intervals, and include electrons scattered from all the materials in the target. The total rate for the full spectrometer acceptance at the central momentum setting p'_0= 4.74 GeV/c (W = 1.49 GeV) is $\sim$ 1000 Hz.

Table 1. Kinematic variables, rates and cross sections.

W	x	Q^2	ϵ	E'	$d^2\sigma/dE'/d\Omega$	Rate	$d^2\sigma$ DIS
[GeV]		[GeV^2]		[GeV]	[nb/(sr GeV)]	[Hz]	[nb/(sr GeV)]
1.170	0.744	1.418	0.960	4.984	69.7	10.1	90.2
1.230	0.689	1.399	0.958	4.918	151.5	21.5	114.5
1.440	0.526	1.325	0.946	4.658	111.1	17.7	150.5
1.530	0.469	1.290	0.940	4.534	172.7	29.2	156.1
1.605	0.426	1.259	0.934	4.426	137.9	24.5	159.1
1.680	0.387	1.226	0.926	4.312	194.1	36.1	160.9
1.930	0.280	1.108	0.893	3.894	165.7	47.2	157.0

The number of counts needed for a given statistical uncertainty ($\delta A/A$) in the measured asymmetries $A_{||}$ and $A_{\perp}$ is given by

$$N = \frac{1}{(f P_b P_t A_{||}(\delta A/A))^2}, \tag{14}$$

where P_b and P_t are the beam and target polarizations. Conversely, a data taking run of fixed duration $t = N/R$ determines the magnitude of ($\delta A/A$). We have chosen the latter approach. For the main momentum setting ($W = M$ to 1.71 GeV) we fixed t = 40 hours of beam with $P_b = 80\%$, on a $^{15}NH_3$ target with average longitudinal $P_H = 85\%$, and t = 60 h on $^{15}ND_3$, with the same beam polarization, and $P_D = 30\%$. A second momentum setting is needed (1.47 GeV$\leq W \leq$ 2 GeV) to cover the full resonances' range. For this setting t = 20 hours for protons and t = 30 hours for deuterons is sufficient because the rates increase with W.

$A_{||}$ was modeled taking as input the results from ref. [5] for $Q^2 \simeq$ 1.2 GeV^2, which are close to our kinematical conditions, without modification. For the regions of x not measured in that experiment, we took the weighted average of $A_{||}$ over the measured range. This is a reasonable estimate in view of the very large errors of these data, which severely restrict any

detailed modeling. Fig. 5 displays a plot combining the values of $A_1+\eta A_2$, the depolarization factor D and $A_{||} = D(A_1 + \eta A_2)$.

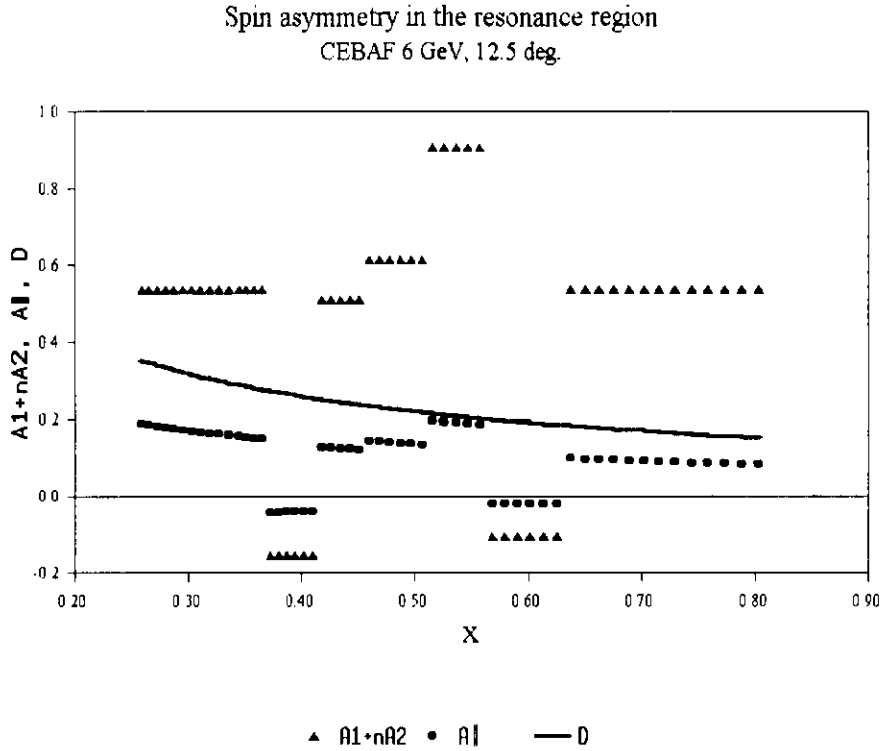

FIG. 5. $A_1 + \eta A_2$ measured in SLAC E130 (triangles), the depolarization D and the resulting $A_{||}$ used as model (circles).

The expected results for the proton are shown in fig. 6. and those for the deuteron in fig. 7. We have used the same $A_1+\eta A_2$ model for both proton and deuteron, in the absence of deuteron data (except for the forthcoming E143 results). This choice is supported in part by the results obtained for A_1^d in the DIS region [10,39], which show this asymmetry approaching 1 at high x, just like the proton's.

For the high Q^2 measurements, we assume the same values for the luminosity, spectrometer solid angle, and beam and target polarizations. The dilution factor can be improved somewhat to $f \approx 0.155$ by using $^{14}NH_3$ since the neutron polarization in ^{14}N is not a problem for this measurement, as it is for A_1^p. The invariant mass interval can be relaxed to $\Delta W = 30$ MeV, doubling the effective counting rate relative to the A_1, A_2 conditions. For fixed data taking time $t \sim 150$ hours, the statistical error in the asymmetry A_{TT} is 0.15.

This precision can be improved to 0.1 (or the time reduced by one half) if the promising polarized target material ^{6}LiD becomes available before the run.

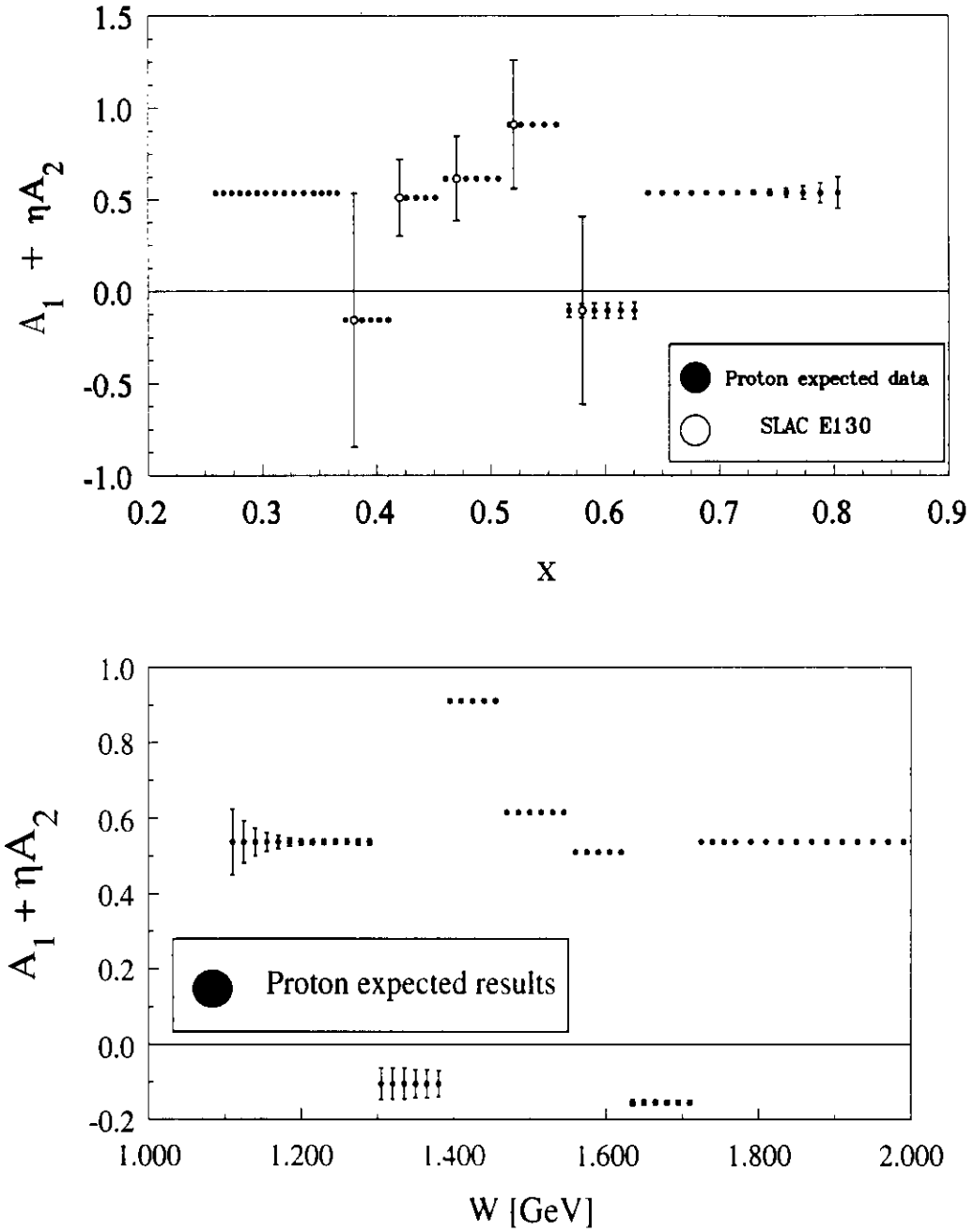

FIG. 6. Expected results for the proton plotted alongside the currently available data vs x (top) and vs W (bottom).

7. Transverse asymmetry.

The separation of the two asymmetries A_1 and A_2 requires a measurement of the transverse asymmetry $A_\perp$. This is a necessary condition to understand the spin asymmetries in more depth than just stating the positivity limit $|A_2| \leq R$, which seems to be marginally obeyed in DIS at high x [12]. Taking data in the transverse target field configuration for one half of the time devoted to the longitudinal configuration, will reduce the errors in A_1 due to $A_\perp$ to a negligible contribution (a 14% average increase in the statistical errors of A_1), and will increase our knowledge of A_2 infinitely. Taking data for a shorter time may not be efficient, considering the overhead involved.

Transverse runs during E143 did not present any unforeseen complications. A chicane is required to compensate for the beam deflection due to the target field, just as is being planned for experiments CEBAF 93-026 and 93-028 mentioned above. The higher beam energy of this proposal compared to the ones planned for those Hall C experiments, simplifies somewhat the requirements, since smaller vertical deflections are involved, both for the incident as well as the scattered electrons. The rotation of the target from the longitudinal to the transverse field orientation was done in less than one 8 hour shift, with the magnet at liquid He temperature.

For the measurement of A_{TT}, the target field has to be oriented along the three-momentum transfer $\mathbf{q}$ vector. At the chosen kinematics, this vector ranges from 15° at $W = 2$ GeV to 21.4° at the Δ. The optimum orientation will be chosen based on the constraints presented by the actual effective angular clearance of the target magnet in the forward direction (nominally $\pm$ 50° relative to the magnet axis).

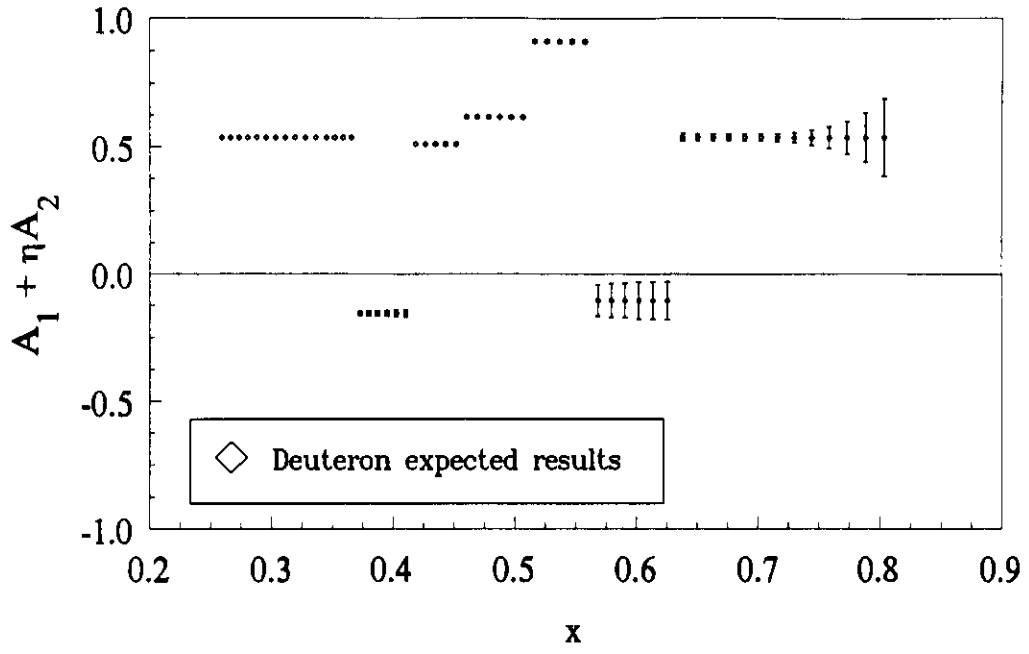

FIG. 7. Expected results for the deuteron plotted vs x.

8. Sources of Systematic Error

The systematic errors involved in spin asymmetry studies come mainly from the nature of the beam and target used. A growing number of experiments (SLAC E80, E130, E142, E143 and E154, CERN EMC and SMC, HERA HERMES) using polarization degrees of freedom have studied in great detail these and other sources of error. The table below gives conservative estimates of the most significant sources of error expected in the present proposal.

Essentially the same systematic errors are present for both the low and high Q^2 parts of the experiment.

Table 2. Sources of systematic error		
Source	**Proton**	**Deuteron**
Beam P_b	2%	2%
Target P_t	2.5%	4%
Dilution f	2%	2%
Nitrogen correction	$< 1\%$	1%
Pion contamination	$< 1\%$	$< 1\%$
Dead time	$< 1\%$	$< 1\%$
Radiative corrections	2%	6%
Errors from R and F_2	3%	3%
Total	5.5%	8.5%

9. Run Plan and Beam Time Request

The running time and experimental conditions described earlier are summarized in table 3 below. The fourth column is the central momentum setting of the HMS, and the fifth column is the invariant mass range that the HMS can cover at that setting. The times are net beam hours. An additional 125 hours for overhead (annealing, Møller and target empty runs and target field rotation) and contingency is included, assuming an 80% efficiency of the combined accelerator operation and experiment data taking.

Experience with the polarized target operation during E143 indicates that data can be taken for periods of 8 to 10 hours with NH_3 and $\sim$ 16 hours with ND_3 before radiation damage reduces the polarization to a level that is too low for efficient data collection. The polarization is restored by annealing the material to about 80 K, in about one hour. Time for 10 anneal cycles is included in the overhead.

The polarization of the beam will be measured at every target change (10-16 hours). About 25 Møller runs (each one hour long) are also included.

Table 3. Run Times and experimental conditions.					
Scattering angle	**B_t Orientation**	**Target**	p_o GeV/c	**Wl- Wh** GeV	**Time** hours
12.5°	Longitudinal	NH_3	4.737	0.938 - 1.710	40
		ND_3			60
		NH_3	4.206	1.470 - 2.000	20
		ND_3			30
Subtotal longitudinal					150
	Transverse	NH_3	4.737	0.938 - 1.710	20
		ND_3			30
		NH_3	4.206	1.470 - 2.000	10
		ND_3			15
Subtotal transverse					75
Subtotal low Q^2 (12.5°)					225
35 °	15° w.r. beam	NH_3	4.589	1.11-1.83	154
Overhead and contingency 33%					125
Total					504

The total request is 21 calendar days.

10. Prospects for improvement before the run

The future availability of more advanced target materials, such as ^{6}LiD, obviously enhances the possibility of further polarized target experiments at CEBAF. LiD has been shown to polarize up to 70% for each nuclear species, in a 6.5 T magnetic field. [40]. The ^{6}Li nuclear structure consists, to a good approximation, of an α particle and a deuteron bound system. Therefore, for inelastic scattering ^{6}LiD behaves like two polarized deuterons, with a 50% fraction of polarized nucleons, i.e. a dilution factor of one half. This is a very attractive combination for experiments which are indifferent to scattering from a polarized proton or neutron (such as Δ production), or exclusive experiments, for which the final state particles

are relevant.

The feasibility of carrying out studies at higher values of the momentum transfer is significantly increased with LiD, because the large dilution factor compensates the lower count rates expected at high Q^2. Our group is intent in testing the properties of LiD in the conditions of our target (5 T magnetic field at 1 K), for possible applications at SLAC (studies of the gluon polarization from J/ψ leptonic decays) and at CEBAF (this proposal). The material is being obtained from two sources (Loa Alamos and Livermore National Laboratories). LiD (like ammonia) needs to be irradiated at low temperature (180 K) so paramagnetic centers are created to transfer the electron polarization to the nuclei. The irradiation will take place at Stanford University's 20 MeV accelerator. The tests will be carried out this spring at UVA's test facility.

REFERENCES

[1] E154 collaboration, R. Arnold *et al.* , *Spin Structure Function Using a Polarized HE-3 Target*, SLAC-PROPOSAL-E-154 (1993).

[2] E155 collaboration, R. Arnold *et al.* , *Measurements of Nucleon Spin Structure at SLAC in End Station A*, SLAC-PROPOSAL-E-155 (1993).

[3] SMC collaboration, *Measurements of the Spin-Dependent Structure Functions of the Neutron and the Proton*, Addendum to the NA47 Proposal, CERN/SPSLC 94-13.

[4] M. Dueren and K. Rith *Polarized Electron Nucleon Scattering at HERA: The HERMES Experiment*, in *Hamburg 1991, Proceedings, Physics at HERA, vol. 1* 427-445.

[5] SLAC E130, G. Baum *et al.*, Phys. Rev. Lett. **45**, 2000 (1980).

[6] SLAC E80, M. J. Alguard *et al.*, Phys. Rev. Lett. **37**, 1261 (1976); **41**, 70 (1978).

[7] SLAC E130, G. Baum *et al.*, Phys. Rev. Lett. **51**, 1135 (1983).

[8] SLAC E142, P. L. Anthony *et al.*, Phys. Rev. Lett. **71**, 959 (1993).

[9] SLAC E143, K. Abe *et al.*, Phys. Rev. Lett. **74**, 346 (1995).

[10] SLAC E143, K. Abe *et al.*, Phys. Rev. Lett. **75**, 25 (1995).

[11] SLAC E143, K. Abe *et al.*, SLAC-PUB-6997 (1994), to be published in Phys. Lett. B

[12] SLAC E143, K. Abe *et al.*, SLAC-PUB-6982 (1994), to be published in Phys. Rev. Lett.

[13] SMC, D. Adams *et al.*,, Phys. Lett. **B329**, 399 (1994).

[14] SMC, B. Adeva *et al.*, Phys. Lett. **B302**, 533 (1993); SMC, B. Adeva *et al.*, Phys. Lett. **B357**, 248 (1995).

[15] J. D. Bjorken, Phys. Rev. **148**, 1467 (1966); Phys. Rev. D **1**, 1376 (1970).

[16] S.J. Brodsky, M. Burkardt and I. Schmidt, report No. SLAC-PUB-6087 (1994)

[17] E.D. Bloom and F.J. Gilman, Phys. Rev. Lett. **25**, 1140 (1970); Phys. Rev. D**4**, 2901 (1971).

[18] R. L. Jaffe and Xiangdong Ji, Phys. Rev. **D43**, 726 (1991).

[19] J. L. Cortes, B. Pire and J. P. Ralston, Z. Phys. **C55**, 409 (1992).

[20] SMC, D. Adams, *et al.*, Phys. Lett. **B336**, 125 (1994).

[21] D. Day, spokesman, *The Charge Form Factor of the Neutron*, CEBAF Experiment 93-026.

[22] J. Jourdan, spokesman, *Deformation of the Nucleon*, CEBAF Experiment 93-028.

[23] G. G. Petratos *et al.*, Report No. SLAC-PUB-5678 (1991).

[24] V.D. Burkert and B.L. Ioffe, *et al.*, Phys. Lett. **B296**, 223 (1992).

[25] V. Burkert, D. Crabb, R. Minehart, spokespersons, *Measurement of Polarized Structure Functions in Inelastic Electron Proton Scattering using CLAS*, CEBAF Experiment 91-023.

[26] S.E. Kuhn, spokesperson, *The Polarized Structure Function Gln and the Q dependence of the Gerasimov-Drell-Hearn Sum Rule for the Neutron*, CEBAF Experiment 93-009.

[27] G. Cates and Z-E. Meziani, spokespersons *Measurement of the Neutron (He) Spin Structure Function at Low Q^2: a Connection between the Bjorken and Drell- Hearn-Gerasimov Sum Rules*, CEBAF experiment 94-010.

[28] C. Carlson, Phys. Rev. D**45**, 2704 (1986).

[29] C. E. Carlson and Wu-Ki Tung, Phys. Rev. D**5**, 721 (1972).

[30] A. J. G. Hey and J. E. Mandula, Phys. Rev. D**5**, 2610 (1972).

[31] P. Stoler, Phys. Rev. Lett. **66**, 1003 (1991); Phys. Rev. D**44**, 73 (1991).

[32] L.M. Stuart, *et al.* , Report No. SLAC-PUB-6316 (1993).

[33] P. Stoler, V. Burkert, M. Taiuti, spokespersons, *The Study of Excited Baryons at High Momentum Transfer with the CLAS Spectrometer*, CEBAF Experiment 91-002.

[34] J. Napolitano*, P. Stoler, spokespersons, *The delta(1232) form Factor at High Momentum Transfer*, CEBAF Experiment 94-014.

[35] F. W. Brasse *et al.* , Nucl. Phys. **B110** (1976) 413.

[36] D. Day, private communication.

[37] L. W. Whitlow *et al.*, Phys. Lett. **B250**, 193 (1990).

[38] L. W. Whitlow *et al.*, Phys. Lett. **B282**, 475 (1992).

[39] T.J. Liu, Doctoral dissertation, Univ. of Virginia, January 1996

[40] A. Abragam, Proc. Int. Symp. on High Energy Phys. with Polarized Beams and Polarized Targets, 1978, Argonne. AIP Conference Proceedings 1979; V. Bouffard *et al.* , J. Physique **12**, 1447 (1980).

APPENDIX

Studying PQCD with Polarized Beams and Targets

PQCD prediction: Hadron *helicity* is conserved

Specific example: $\Delta_{(1232)}$ electroproduction at high energy.

3 helicity amplitudes: (Breit frame)

G_+: $N_{1/2} + \gamma_1 \rightarrow \Delta_{1/2}$

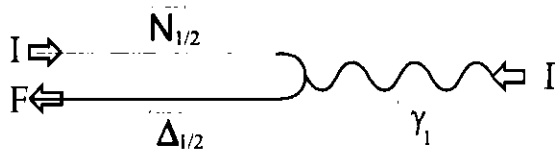

G_0: $N_{1/2} + \gamma_0 \rightarrow \Delta_{-1/2}$

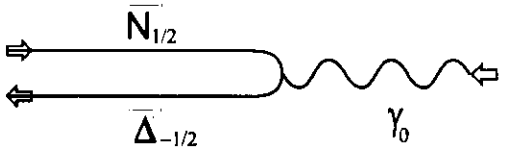

G_-: $N_{1/2} + \gamma_{-1} \rightarrow \Delta_{-3/2}$

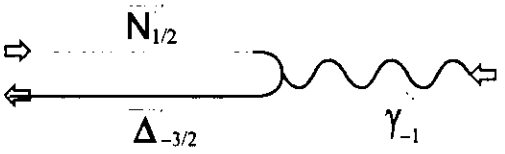

QCD says:

G_0 adds an m/Q term to G_+ ($\sim 1/Q^3$), flip 1 spin.

G_- " $(m/Q)^2$ " " 2 "

Therefore at high Q^2 $G_- << G_0 << G_+$

In terms of multipole amplitudes:

$G_+ = \sqrt{4\pi}\,(M_1 + \sqrt{3}\,E_2)/2$

$G_- = \sqrt{4\pi}\,(-\sqrt{3}M_1 + E_2)/2 \overset{Q^2\rightarrow\infty}{=} 0 \Rightarrow E_2 = \sqrt{3}\,M_1$

$G_0 = \sqrt{4\pi}\;\; Q/|q|\; C_2 \overset{Q^2\rightarrow\infty}{=} 0$

From G_+ to the $G^*_M(Q^2)$ form factor

The cross section for Δ electroproduction is

$$\frac{d\sigma}{d\Omega dE'} = \Gamma_T \frac{4\alpha\pi(\nu^2 + Q^2)}{\Gamma_R m_\Delta (m_\Delta^2 - m_N^2)} G^{*2}_M(Q^2)$$

where Γ_T is the virtual photon flux factor, and

$G^*_M(Q^2)$ is the Δ transition from factor.

The connection between G^*_M and the helicity amplitudes $G_{+,-,0}$ was made by Carlson [Phys. Rev. D34 (1986) 2704]:

$$G^{*2}_M(Q^2) = \frac{2m_N^2}{\nu^2 + Q^2}(G^2_+ + G^2_- + 2\varepsilon G^2_0)$$

which as $Q^2 \to \infty$ become

$$G^*_M(Q^2) = \frac{\sqrt{8}\, m_N^2}{Q^2} G_+ \sim 1/Q^5$$

The ratio of G^*_M to the nucleon dipole form $G_D = 3/(1+ Q^2/0.71)^2$ at high Q^2 should be ~ $1/Q$, so

$$Q^2 (G^*_M/G_D)^2 \sim \textit{constant}, \quad \text{as } Q^2 \to \infty$$

Polarized Δ electroproduction on NH_3 or ND_3

e-p scattering => Δ^+ => π^0 p
π^+ n

e-n scattering => Δ^0 => π^- p
π^0 n

} Both have equal σ

$$\frac{d^2\sigma_{e\text{-}nucleus}}{d\Omega dE'} = \frac{d\Sigma}{d\Omega} + f P_b P_t \frac{d\Delta}{d\Omega}$$

f = dilution

P_b, P_t = beam, target pol.

$$\frac{d\Sigma}{d\Omega} = K(G_0^2 + k_U(G_+^2 + G_-^2))$$

$$\frac{d\Delta}{d\Omega} = K(k_L \sin\theta_N \cos\phi_N G_0 G_+ + k_T \cos\theta_N (G_-^2 - G_+^2))$$

where K, k_U, k_T, k_L are kinematics terms

θ_N = in-plane target polarization orientation relative to **q**

We want $\theta_N = 0$, $\phi_N = 0$ to extract G_-^2

$$\frac{d\Delta/d\Omega}{d\Sigma/d\Omega} = \frac{k_T(G_-^2 - G_+^2)}{G_0^2 + k_U(G_+^2 + G_-^2)} \overset{Q^2 \Rightarrow \infty}{=} \frac{-k_T G_+^2}{k_U G_+^2} = \frac{-k_T}{k_U}$$

In terms of multipoles: ($Q^2 \Rightarrow \infty$, $E_2 = \sqrt{3}\, M_1$, $C_2 = 0$)

$$\frac{d\Delta/d\Omega}{d\Sigma/d\Omega} \Rightarrow A_{TT} = \frac{M_1^2 - E_2^2 - 6\mathrm{Re}(E_2^* M_1/\sqrt{3})}{k_L C_2^2 + 2M_1^2 + 2E_2^2} = -1$$

Proposed measurement

Measure $\frac{d\Delta/d\Omega\, k_U}{d\Sigma/d\Omega\, k_T}$ = -1 to ~10% statistical precision

Use $^{14}NH_3$ (f = 17% in the Δ region)
$^{14}ND_3$ (f = 30%); ^{6}LiD (f = 50%)

Kinematics (CEBAF)

Beam energy E = 6 GeV
Scattering angle $\theta_e = 35°$ $Q^2 = 5.7$ GeV^2
$\theta_q = 21.4°$ $\theta_e + \theta_q = 56.4° > 50°$ (magnet opening)
Using $\theta_N = -6.4°$ (target angle w. r. t. **q**; $\theta_{N\text{-beam}} = 15°$)
Contamination from G_0 G_+ contribution:

(k_L / k_T) sin 6.4° $(G_0 / G_+)[5.7\ \text{GeV}^2] < 0.5\%$